Nanoscale Advances

ROYAL SOCIETY OF CHEMISTRY

PAPER

View Article Online
View Journal | View Issue

Cite this: *Nanoscale Adv.*, 2021, **3**, 6063

A β-cyclodextrin enhanced polyethylene terephthalate film with improved contact charging ability in a high humidity environment†

Nannan Wang,‡[ab] Yizhe Liu,‡[ab] Yang Wu,[c] Zibiao Li *[de] and Daoai Wang *[ac]

Moisture in the environment can severely decrease the contact charging properties of polymers, which usually reduce the output of solid–solid triboelectric nanogenerators (TENGs), hindering their further practical applications. To solve this problem, in this paper we fabricated a new type of polyethylene terephthalate (PET) based TENG, which can work stably in a high humidity environment with high output performance. The surface of the PET film is modified with β-cyclodextrin to introduce hydroxyl groups, which increase the ability to form hydrogen bonds with water molecules in a high humidity environment, immobilizing water molecules to participate in contact charging. Since water molecules are a more positive material, the PET film combined with water molecules will acquire more positive charges during the contact charging process, which will greatly increase the electrical output of PET-based TENGs. Different from the PET film-based TENG without hydroxyl on the surface, the electrical output of the β-cyclodextrin-modified PET-based TENG increases with the increase of environmental humidity. The circuit current (I_{sc}) of the TENG increases from 3.7 μA to 16 μA when the humidity increases from 15% to 95%. Moreover, the dielectric properties of the PET film increase due to the introduction of amino groups in β-cyclodextrin, which causes the I_{sc} of the TENG to increase by 3.7 times at 15% RH. This strategy highly expands the application scope of TENGs for energy harvesting and self-powered sensors in high humidity environments, especially in cloudy and foggy days or under water and sweat conditions.

Received 11th May 2021
Accepted 24th August 2021

DOI: 10.1039/d1na00341k

rsc.li/nanoscale-advances

Introduction

With the consumption of non-renewable energy sources and the rapid increase in the number of portable electronic devices, the development of technologies related to energy storage is crucial. Since the birth of the first triboelectric nanogenerator (TENG) in 2012,[1] due to its wide range of energy sources,[2,3] low cost,[4,5] and strong reliability,[6–8] more and more attention has been focused on this type of energy harvesting device. However, the water molecules in a high humidity environment seriously affect the application of TENGs.[9–12] Especially for solid–solid TENGs, the environmental humidity has a significant effect on their output performance owing to different friction charge generating rates at various humidities, for example, when the humidity

[a]*State Key Laboratory of Solid Lubrication, Lanzhou Institute of Chemical Physics, Chinese Academy of Sciences, Lanzhou 730000, China. E-mail: wangda@licp.cas.cn; Tel: +86-931-4968169*

[b]*Center of Materials Sciences and Opto-Electronic Technology, University of Chinese Academy of Sciences, Beijing, 100049, China*

[c]*Qingdao Center of Resource Chemistry and New Materials, Qingdao 266100, China*

[d]*Institute of Materials Research and Engineering, A*STAR (Agency for Science, Technology and Research), 2 Fusionopolis Way, Innovis, #08-03, Singapore 138634, Singapore. E-mail: lizb@imre.a-star.edu.sg*

[e]*Department of Materials Science and Engineering, National University of Singapore, Singapore 117575, Singapore*

† Electronic supplementary information (ESI) available. See DOI: 10.1039/d1na00341k

‡ These authors contributed equally to this work and should be considered co-first authors.

Nannan Wang received his BS (2015) in Pharmaceutical Engineering from Guizhou University. He is currently studying in the State Key Laboratory of Solid Lubrication, Lanzhou Institute of Chemical Physics (LICP), Chinese Academy of Sciences (CAS). He mainly focuses on the research of fabrication of triboelectric nanogenerators and nano devices.

Yizhe Liu received his BS (2018) in Chemical Engineering and Technology from China University of Petroleum (East China). He is currently studying in the State Key Laboratory of Solid Lubrication, Lanzhou Institute of Chemical Physics (LICP), Chinese Academy of Sciences (CAS). He mainly focuses on the research of fabrication of supramolecular aqueous lubricating materials.

increased from 15% to 90%, the triboelectric output of aluminum (Al) and polyvinylidene fluoride (PVDF) decreased by 65.4%,[13] which not only affects the energy collection efficiency and working reliability of TENGs, but also greatly reduces their practical application ranges, especially in areas with high humidity. Generally speaking, the factors that affect the electrical output of TENGs include the dielectric property and triboelectricity of the material,[14,15] the structure of the surface,[16,17] the thickness of the material,[18,19] and the temperature,[20] humidity[21] and atmosphere[22,23] of the environment, and so on. In terms of environmental humidity, water molecules in the environment adhere to the surface of the friction layer, resulting in a decrease in the amount of triboelectricity between the polymers;[24,25] at the same time, the migration of water molecules will carry the charges on the surface of the friction layer to the environment, resulting in polymer degradation, so the dissipation of surface charge increases.[26,27]

Several approaches have been developed to improve the electrical output performance of the triboelectric nanogenerators in high humidity, including sealing the TENG to isolate water molecules,[28–30] using hydrophobic or superhydrophobic materials to reduce the adsorption of water molecules on the friction surface,[31,32] or using loose structures to increase the permeability of the material. However, these methods involving the use of encapsulating or hydrophobic friction electrodes in TENGs are cumbersome and complex, and are not easy to implement for some materials and large-scale applications. Moreover, these methods cannot completely reverse the decreasing trend of humidity on the performance of TENGs. Therefore, from the point of view of material design, there is an urgent need to fundamentally improve the moisture resistance at the friction interface and design a new type of TENG with high output performance in high humidity to improve the adaptability of the friction nanogenerator.

In our previous work, we introduced a bio-based triboelectric nanogenerator that can work stably in a high-humidity environment.[33,34] Hydroxyl-rich bio-based materials can fix water molecules in the environment to participate in triboelectricity, thereby increasing the electrical output of bio-based TENGs in a high-humidity environment. Inspired by this, in this article we modified β-cyclodextrin on the surface of the polyethylene terephthalate (PET) film to introduce hydroxyl groups. The hydroxyl groups on the surface of the PET film can form hydrogen bonds with water molecules in the environment, making water molecules participate in triboelectricity as a more positive material, which will increase the electrical output of the PET-based TENG in a high-humidity environment. The results show that the circuit current (I_{sc}) of the TENG increases 3.3 times when the humidity increases from 15% to 95%. Moreover, the dielectric properties of the PET film increase due to the introduction of amino groups in β-cyclodextrin, which causes the I_{sc} of the TENG to increase 3.7 times at 15% RH. This strategy highly expands the application scope of TENGs for energy harvesting and self-powered sensors in high humidity environments, especially in cloudy and foggy days or under water and sweat conditions.

Experimental

Materials

Polyethylene terephthalate (PET, thickness 0.1 mm) was purchased from Dongguan Le Rui Plastic Co., Ltd, and γ-glycidoxypropyltrimethoxysilane (KH-560 silane coupling agent) was purchased from Azerbaijan Latin Reagent Company; a polytetrafluoroethylene membrane (PTFE, 0.05 mm) was purchased from Zhenjiang Hongke Rubber and Plastic Co., Ltd, and amino-β-cyclodextrin and *N*,*N*-dimethylformamide were purchased from Sinopharm Reagent Company. Copper tape, copper wires and green LED lights were purchased from a local supermarket. Salts (LiCl, $MgCl_2$, $Mg(NO_3)_2$, NaCl, and KNO_3) were purchased from Macklin, CP and used to control the humidity to 15%, 35%, 55%, 75%, and 95%.

Preparation of a β-cyclodextrin modified PET electrode

First, the PET film was soaked in KH560/methanol (1 wt%) solution for 3 hours. After drying in a wind box at 80 °C for 2 h, the epoxy groups were grafted onto the surface. The polyurethane membrane was immersed in a 10 mg ml^{-1} dichloromethane solution of aminocyclodextrin at 80 °C for 24 h, washed with absolute ethanol 3 times, and dried under nitrogen

Yang Wu received his bachelor's degree from Qufu Normal University, China (2010), and his PhD degree from LICP, CAS, 2015. He has been a research assistant at the City University of Hong Kong (2016–2017). He has published 40 papers and obtained more than 10 patents for invention. Now, he is an associate professor at the State Key Laboratory of Solid Lubrication, LICP, CAS. His research interests mainly focus on aqueous lubrication, underwater adhesion of soft materials and low surface energy coatings.

*Zibiao Li obtained his PhD degree from the National University of Singapore (NUS). Currently, he is working as a research scientist at the Institute of Materials Research and Engineering (IMRE), A*STAR, Singapore. He is the Head of Advanced Sustainable Materials (ASM) Department at IMRE. His research interests are focused on functional polymeric materials design, structural property investigations, and their hybrids for healthcare and consumer care applications.*

Prof. Daoai Wang received his PhD from the Lanzhou Institute of Chemical Physics, CAS. From 2009 to 2010, he worked as a Postdoc in the Max Planck Institute of Microstructure Physics. From 2010 to 2013, he worked as a JSPS researcher in the University of Tokyo. And he is now a professor in LICP supported by the ''Top Hundred Talents'' Program of Chinese Academy of Sciences. His research interests include triboelectrification and tribology.

flow to obtain a β-cyclodextrin functional surface. Then, the modified PET film was affixed with a conductive copper electrode and a copper wire on the backside to obtain the PET film friction electrode.

Fabrication of a modified PET-based TENG

The modified PET film was affixed with a conductive copper electrode and a copper wire on the backside to obtain the PET film friction electrode. The PTFE film was cut into a size of 4 cm × 4 cm, and a copper electrode was attached to the back with a copper wire to prepare a PTFE film electrode. The PET film electrode and PTFE electrode were assembled into a TENG.

Characterization

The surface topography of the modified PET film was obtained using a commercial atomic force microscope (Dimension Icon, Bruker) in AFM mode. The dielectric constant is tested using a Japanese AET high-frequency dielectric constant tester. The thickness of the PVA sample is 0.1 mm, the area is a square of "4 cm × 4 cm", and the test frequency is 10 GHz. X-ray photoelectron spectroscopy (XPS) spectra were recorded using a Kratos Axis Ultra instrument employing a monochromatic Al Kα source (1486.69 eV), a hemispherical analyser with a hybrid (electrostatic and magnetic) lens system, charge neutralization by filament-generated magnetically channeled low-energy electrons, and a delay line detector (DLD). Fourier transform infrared spectroscopy (FTIR) spectra of the PET film at different humidities were recorded on an FTIR spectrometer (Nicolet 6700, Thermo Fisher Scientific Inc.) from 4000 to 400 cm^{-1} at a resolution of 4 cm^{-1}. The infrared test method of the PET film at different humidities is as follows: place the PET film in a desiccator equipped with saturated salt solution to control different humidities for 24 h, and then put the PET film that was placed at different humidities quickly under the infrared test probe to quickly obtain the infrared curve. To measure the triboelectrification output performance, a commercial linear mechanical motor was used to drive the starch film based TENGs with a contact-separation mode. The output voltage was measured by using a NI PCIe-6259 DAQ card (National Instruments) with a load resistance of 100 MΩ, while the short-circuit current was measured by using an SR570 low-noise current amplifier (Stanford Research System). To test the output of the PET film based TENGs at different humidities, the PET film triboelectrodes were first put into a sealed box for 24 h, where the humidity was adjusted to 15%, 35%, 55%, 75% and 95% by using different saturated salt solution, respectively, and then tested the output performance in the same humidity control box.

Results and discussion

Fig. 1a shows the schematic structure of the β-cyclodextrin modified PET-based TENG. Due to the hydrophobic nature of the PTFE film, water molecules will not accumulate on the surface in a high-humidity environment, which makes PTFE the best negative electrode material for preparing moisture-resistant TENGs. In order to introduce hydroxyl groups on the surface of the PET film, β-CD was modified on the surface, as shown in Fig. 1b. First, the PET film was immersed in KH560/methanol (1 wt%) solution for three hours. After drying at 80 °C in an air oven for 2 h, the epoxy group was modified on the surface. Then, the PET film was immersed in the 10 mg ml^{-1} DMF solution of amino cyclodextrin at 80 °C for 24 h and washed with anhydrous ethanol three times, and dried under N_2 flow to obtain a CD functional surface. Hydroxyl and amino groups are introduced on the surface of the modified PET film, which will have a huge impact on the electrical output of the PET-based TENG. To check whether β-CD is modified on the surface, the XPS spectra of the blank and the modified PET film were recorded, as shown in Fig. 1c and d. The results showed that compared with the blank PET film, the modified PET film showed absorption peaks of Si and N at 102 eV and 399 eV, indicating that HK560 and β-CD were successfully modified on the surface of the PET film. Moreover, the infrared spectra of blank PET and modified PET films were recorded, as shown in Fig. S1.† In the IR spectrum of pure PET, the characteristic absorption peak of the C–O bond is at 1080 cm^{-1}, while in the infrared spectrum of the modified PET, the double peaks at 1100 cm^{-1} and 1080 cm^{-1} are the characteristic absorption peaks of Si–O–C, which mask the C–O absorption peak of the PET molecule, indicating that KH560 is successfully modified on the surface of PET (KH560 contains the Si–O bond). In addition, in the infrared spectrum of modified PET, the characteristic absorption peak of –OH at 3416 cm^{-1} indicates that β-CD has been modified on the surface of PET. Then, EDS of the two PET films was performed, as shown in Fig. S2 and S3.† The results show that the pure PET film only shows the Kα absorption peaks of C and O elements at 0.27 eV and 0.52 eV. However, the modified PET film showed the Kα absorption peak of the N element at 0.39 eV, and the Kα and Kβ absorption peaks of the Si element at 1.74 eV and 1.84 eV, respectively, indicating the existence of amino-β-CD and KH560 on the PET surface. Furthermore, the contact angle test results (insets of Fig. 1c and d) show that after modification, the contact angle of the PET film decreased from 73° to 32°, indicating that the hydrophilicity of the PET film increases and hydroxyl groups are introduced on the surface. Then, the AFM photos of the blank and modified PET films were analyzed to more intuitively characterize that β-CD was successfully modified on the surface, as shown in Fig. 1e and f. Compared with the blank film, a large number of bright yellow dots appeared on the surface of the modified PET film, indicating that β-CD was modified on the surface.

The position of the β-CD modified PET film (β-CD@PET) in the triboelectric polarity sequence is shown in Fig. 2a. In the process of testing, the PTFE electrode was used as the friction electrode, and the counter electrode was selected from aluminum (Al), β-CD@PET, blank PET, polystyrene (PS), and polydimethylsiloxane (PDMS) to form the TENG. The results show that the short-circuit current (I_{sc}) of the TENG composed of β-CD and PTFE was between that of Al- and PET-based TENGs, indicating that β-CD is an electropositive material, and the tribo-electrode is between Al and PET. Fig. 2b shows the

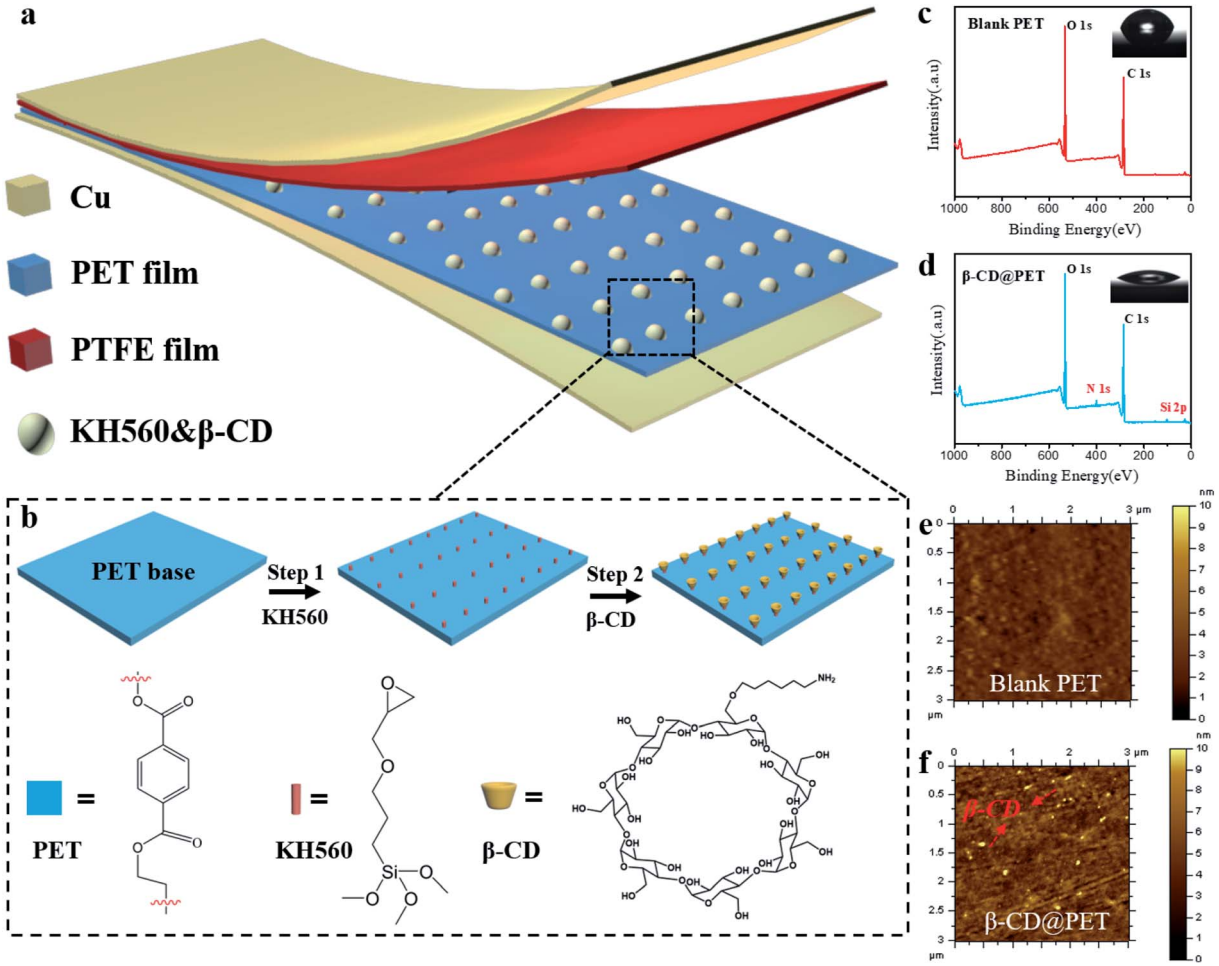

Fig. 1 Schematic diagram of the (a) modified PET based-TENG and (b) β-cyclodextrin (β-CD) modified PET film. The XPS spectrum and contact angle of the (c) blank PET film and (d) modified PET film. AFM photos of the (e) blank PET film and (f) modified PET film.

working mechanism of the PET-based TENG. Generally, the generation of triboelectric charge of the TENG is ascribed to the coupling effect of triboelectrification and electrostatic induction. When the PET and PTFE layers are pressed to come into contact, positive charges generate on the surface of PET and negative charges generate on the surface of PTFE (Fig. 2b-i). When the PET and PTFE layers are separated from each other, a potential difference between the PET and PTFE layers drives electrons from the copper back electrode of PTFE to the PET electrode due to the electrostatic induction, and thus the current flows from the PET/Cu electrode to the PTFE/Cu electrode (Fig. 2b-ii) and the Cu layer on the back of PET generates negative charges, and the Cu layer on the back of PTFE generates positive charges at the same time. Once the charges reach a balanced state, no current flows in the circuit (Fig. 2b-iii). Similarly, during the pressing process, a reverse current is detected from the PTFE/Cu electrode to the PET/Cu electrode (Fig. 2b-iv). With the coupling of contact electrification and electrostatic induction, electricity is generated alternately while the TENG experiences a contact-separation process.

Fig. 3 shows the comparison of electrical output between blank PET- and β-CD@PET-based TENGs. As a traditional polymer material, the I_{sc} of the blank PET-based TENG decreased with the increase of humidity (Fig. 3a). When humidity increased from 15% to 95%, the I_{sc} of the PET-based TENG decreased from 1.0 μA to 0.1 μA with a decrease of 90%. In addition, the V_{oc} of the PET-based TENG decreased from 17.7 V to 1.5 V with a decrease of 91%. Contrary to the variation of the I_{sc} of the blank PET-based TENG with humidity, the I_{sc} of the β-CD@PET-based TENG increased with the increase of humidity. As shown in Fig. 3d, when humidity increased from 15% to 95%, the I_{sc} of the β-CD-based TENG increased from 3.7 μA to 15.9 μA with an increase of 329%. At the same time, the V_{oc} of the β-CD@PET-based TENG was calculated, as shown in Fig. 3e. Similarly, the V_{oc} increased with the increase of humidity and when the humidity increased from 15% to 95%, the V_{oc} increased by 4.8 times. Then, to characterize the impact of dynamic humidity on the electrical output performance of these two TENGs, we determined the real-time short-circuit currents of TENGs in a closed box with continuous water vapor. As shown in Fig. 3c and f, water vapor was continuously supplied to a closed box to continuously increase the humidity in the closed box, and the I_{sc} of the two TENGs was continuously measured during this process. The results show

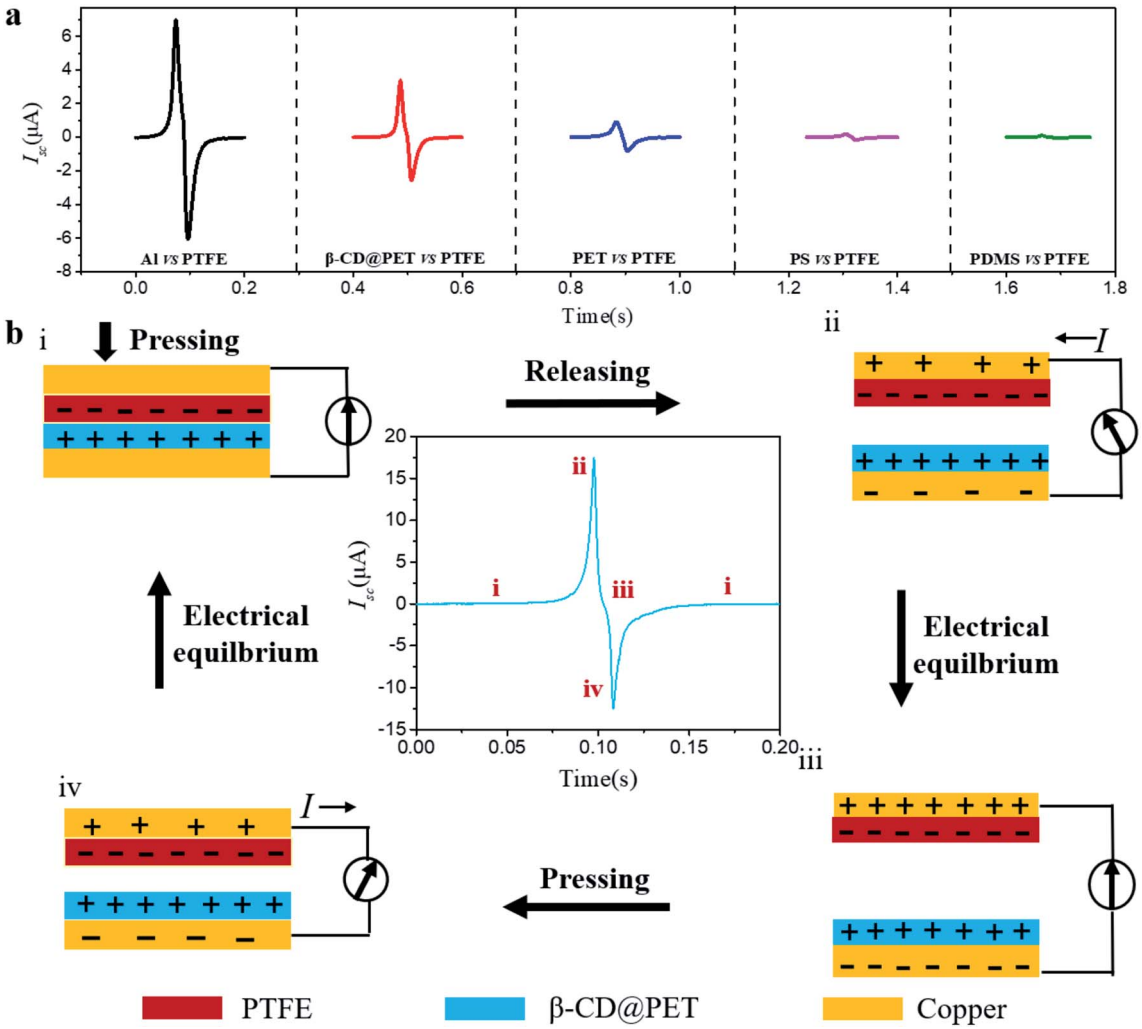

Fig. 2 (a) The position of the β-CD modified PET film (β-CD@PET) in the triboelectric polarity sequence. (b) The working mechanism of the PET-based TENG.

that the I_{sc} of the blank PET-based TENG decreased from 1.18 μA to 0.16 μA, while the I_{sc} of the β-CD@PET-based TENG increased from 5.1 μA to 14.9 μA, and this finding is consistent with the above results. Then, I_{sc} and V_o at two extreme humidities of 15% RH and 95% RH were chosen respectively for comparison, as shown in Fig. S4.† At 15% RH, I_{sc} and V_o of the modified PET-based TENG are 3.6 times and 3.9 times higher than that of the blank PET-based TENG, respectively. When the humidity increases to 95%, the electrical output gap between the modified PET-based TENG and the blank PET-based TENG is further widened. The schematic diagram of the real-time short-circuit current test of TENGs in a closed box is shown in Fig. S5.†

Fig. 4a shows the dependence of I_{sc} and the corresponding power on the external loading resistance of blank PET- and β-CD@PET-based TENGs at a humidity of 55%. The I_{sc} gradually drops with the increase of the resistance due to the ohmic loss, and when the resistance value was 50 MΩ, the β-CD@PET-based TENG had a maximum output power of 1.88 mW at 55% humidity. Similarly, the blank PET-based TENG also exhibits a maximum output power when the load is 50 MΩ, but the value is only 0.24 mW. The variations of the maximum output power (all the maximum powers appear when the load is 50 MΩ) of the β-CD@PET-based TENG and blank PET-based TENG at 15%, 35%, 55%, 75% and 95% humidity are shown in Fig. 3b. For the β-CD@PET-based TENG, the maximum output power increases with the increase of humidity, and the maximum power value increased from 0.81 mW to 5.66 mW, with an increase of 6.9 times, that is, the higher the humidity, the higher the output power. However, the blank PET-based TENG shows an opposite trend (the maximum power value reduced from 0.42 mW to 0.006 mW, with a 70-fold reduction), the higher the humidity, the smaller the output, which is consistent with the change of current and voltage with humidity. In order to cope with the alteration of humidity in practical applications, a dry–wet alternating cycle test was performed to demonstrate that the β-CD@PET-based TENG has excellent reversible properties (Fig. 4c). Interestingly, the β-CD@PET-based TENG could continue to maintain a high output of 15.0 μA at 95% humidity, and a low output of 3.7 μA when humidity was decreased to

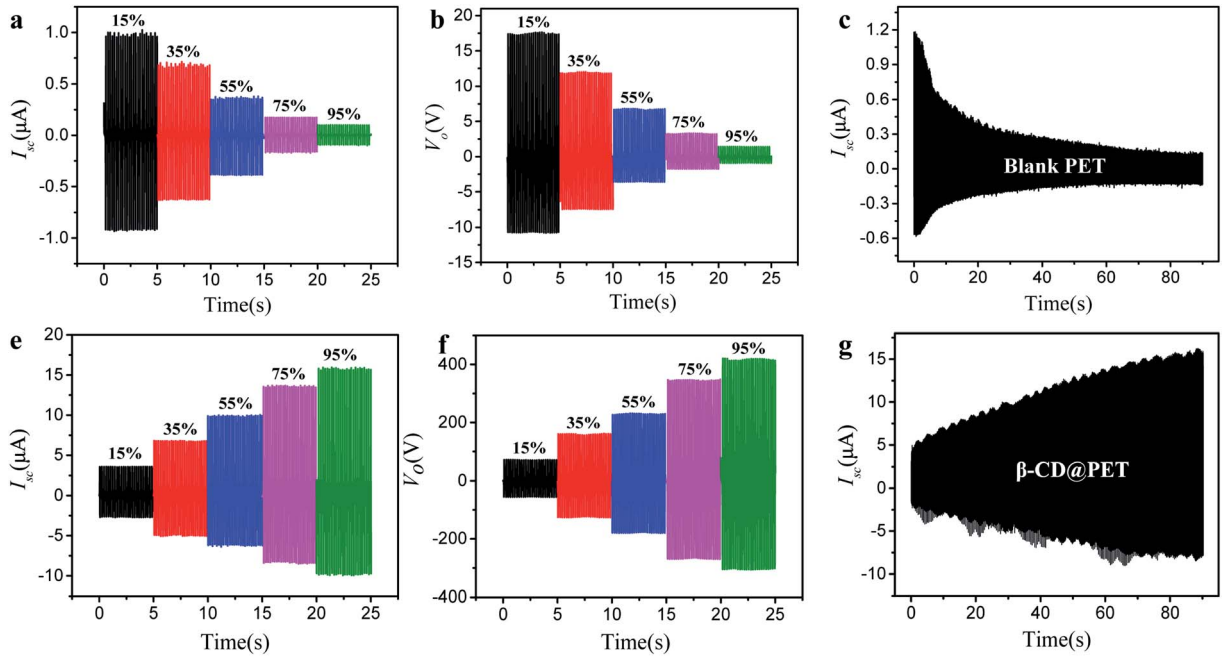

Fig. 3 Effect of humidity on the output performance of blank PET and β-CD-based TENGs. (a) I_{sc} and (b) V_{oc} of the blank PET-based TENG at humidities of 15%, 35%, 55%, 75% and 95%, respectively. (c) The corresponding real-time I_{sc} of the blank PET-based TENG with the continuous humidity change. (d) I_{sc} and (e) V_{oc} of the β-CD PET-based TENG at humidities of 15%, 35%, 55%, 75% and 95%, respectively. (f) The corresponding real-time I_{sc} of the β-CD@PET-based TENG with the continuous humidity change.

15%, while as the humidity increased to 95% again, the output returned to its original high value. After several cycles, the changes in ambient humidity will not cause damage to the output of the β-CD@PET-based-TENG at high humidity. At the same time, in order to ensure a continuous and stable output of the β-CD@PET-based TENG in a high humidity environment, a stability test at an extreme humidity of 95% was performed, which is shown in Fig. 4d. After more than 12 h, the current of the β-CD@PET-based TENG was stable at about 15.1 μA, indicating that the β-CD@PET-based TENG can be stably used as an energy collecting device in a high humidity environment for a long time.

Generally, the triboelectrification state of the friction pairs is restricted by many factors, including the chemical composition and structure of the friction pairs, the friction motion conditions, the device design of the TENG, the environmental temperature, and humidity factors. In the above comparative experiment of β-CD@PET- and blank PET-based TENGs, we strictly controlled the conditions to make two groups of TENGs including the device assembly, friction movement conditions, smooth and flat structure of the material surface, test temperature conditions, and other factors strictly consistent throughout the test while only changing the humidity. Hence, in the test system, the change of triboelectrification performance is mainly caused by the change of environmental humidity. In general, water molecules in the environment participate in inhibiting the friction and electrification of the material surface, thus accelerating the cumulative surface charge dissipation to the environment. However, for the β-CD@PET-based TENG, the experimental results showed an opposite trend, wherein its triboelectrification performance increased with the increase of environmental humidity, indicating that other mechanisms, such as the formation of new substances or functional groups on the surface of β-CD@PET to change its surface polarity, determine this trend. In order to determine the mechanism during this process, the infrared spectrum of the β-CD@PET surface to detect the change of its chemical composition in this process was analyzed, as shown in Fig. 5. To characterize the formation of hydrogen bonds, the IR spectra of the β-CD@PET films from 15% to 95% RH were obtained (Fig. 5a). In the infrared spectrum, the shock absorption peaks of –OH were observed from 3300 cm^{-1} to 3500 cm^{-1}. As the humidity increases, the absorption peak of –OH moved toward a lower wavenumber (red shift). Moreover, the higher the humidity, the larger the wave number of the red shift, indicating the formation of more hydrogen bonds.

Furthermore, to further prove that the change of output current of the β-CD@PET-based TENG at different humidities is caused by the difference in the amount of hydrogen bonds, the IR spectra and I_{sc} of β-CD@PET films which absorb moisture for different times (0, 1, 2, 3, 4, and 5 h) at 95% RH were analyzed, as shown in Fig. 5b and c. As shown in Fig. 5b, the hydroxyl absorption peak of the β-CD@PET film that absorbed water for 1 h shifted from 3428.1 cm^{-1} to 3413.6 cm^{-1} compared with that of the completely dry film that did not absorb water. Correspondingly, the I_{sc} of the β-CD@PET-based TENG that absorbed water for 1 h showed a rapid and substantial increase from 3.8 μA to 6.1 μA compared with that of the dry one (Fig. 5c). As the water absorption time continuously increased from 1 h to 5 h, the wavenumber of the hydroxyl absorption peak moves to

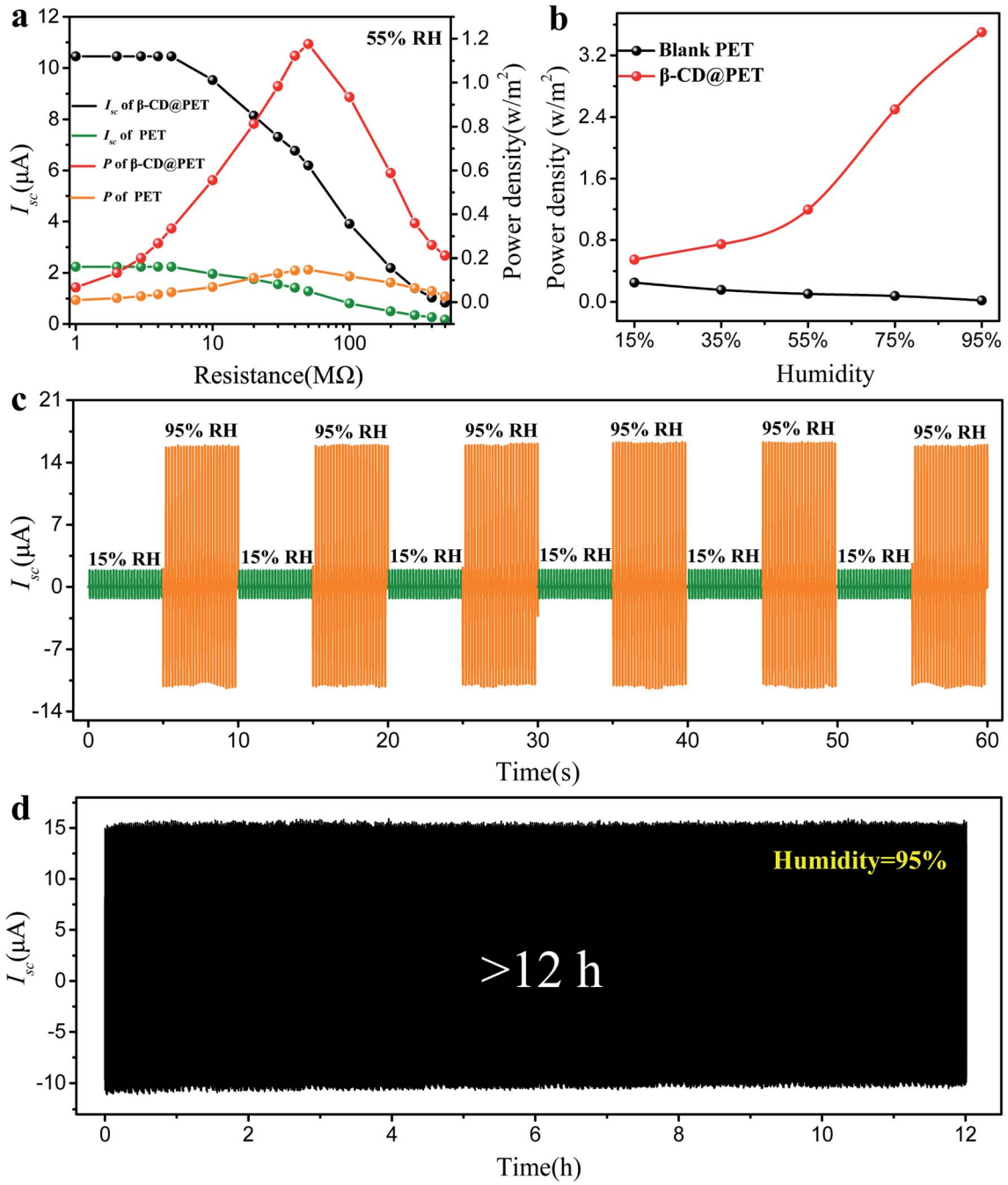

Fig. 4 Output performance, stability and reversible output performance of the β-CD@PET-based TENG. (a) Dependence of I_{sc} and the corresponding power density on the external loading resistance of blank PET- and β-CD@PET-based TENGs at a humidity of 55%, (b) comparison of the output power density of blank PET- and β-CD@PET-based TENGs at humidities from 15% to 95%, (c) reversible output properties of the β-CD@PET-based TENG in an alternating dry (RH 10%) and wet (RH 99%) environment, and (d) stability test of the β-CD@PET-based TENG at 95% RH.

3391.5 cm^{-1}, indicating that the longer the β-CD@PET film absorbs water, the more hydrogen bonds are formed between β-CD and water molecules. Similarly, when the water absorption time increased from 1 h to 5 h, the I_{sc} increased from 6.1 μA to 10.0 μA. The dry β-CD@PET film electrode and the Al electrode were assembled into the TENG, and the initial current and peak shape were measured immediately in 15%, 35%, 55%, 75%, and 95% humidity chambers (Fig. 5d). The results showed that when the humidity changed from 15% to 55%, both peak shapes were down-up peak and the I_{sc} was reduced, but when the humidity changed from 55% to 95%, the peak shapes changed from down-up peak to up-down peak, and the I_{sc} increased at the same time. Hence, when humidity exceeded 75%, the electro-positivity of the β-CD@PET film increased,

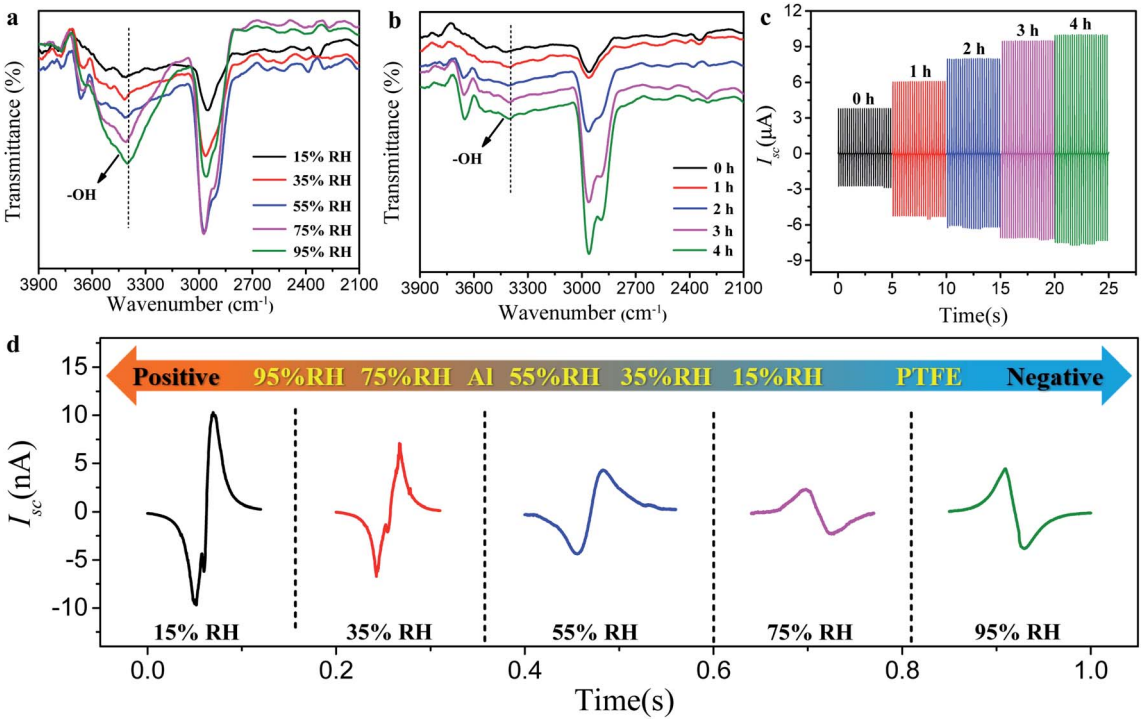

Fig. 5 (a) IR spectra of β-CD@PET films at varying humidities from 15% to 95%, (b) effect of moisture absorption time on IR spectra and (c) output current at 95% humidity for 0 to 5 h, and (d) the value of I_{sc} and peak shape of the β-CD@PET-Al-based TENG at varying humidities.

thus increasing the value of I_{sc}. Therefore, the mechanism that the electrical output of the β-CD@PET-based TENG increases with the increase in humidity is related to the formation of hydrogen bonds, that is, the hydroxyl groups on the surface of the β-CD@PET film form hydrogen bonds with water molecules in the high humidity environment, thereby turning free water into fixed water and making water molecules participate in triboelectricity as an electropositive material. The higher the humidity, the more water molecules will be fixed by β-CD molecules, so the larger the electrical output of the β-CD@PET-based TENG. The mechanism of water molecule immobilization on the β-CD@PET film surface and participation in triboelectric charging is shown in Fig. S6.†

In addition to the reason that the hydroxyl groups on the surface of β-CD@PET fixing water molecules through hydrogen bonds enhance the electropositivity under high humidity, the decrease in the charge dissipation rate caused by strong charge retention ability of β-CD@PET in high humidity environments will also affect the electrical output performances of the β-CD@PET-based TENG under high humidity. As shown in Fig. 6a and b, blank PET- and β-CD@PET-based electrodes were in contact and separated with the PTFE electrode 100 times, respectively, under the operation of motor, and then immediately placed in a closed box with a controlled humidity of 15%. The probe of the surface electrometer was fixed on the opposite side of the blank PET-based electrode with a distance of 2 cm from the film surface, and the real-time surface potential was collected using a computer connected to the surface electrometer (Fig. S7†). The surface potential of the blank PET-based electrode decreased from 122 V to 89 V within 200 s at 15% humidity with a decrease of 33 V; however, the β-CD@PET-based electrode decayed from 122 V to 101 V with a decrease of 21 V. Then, the real-time surface potentials of the two PET films at 95% RH were obtained, as shown in Fig. 6b. The surface potential of the blank PET-based electrode dropped sharply from 120 V to 23 V within 200 s at 95% humidity, while for the β-CD@PET-based electrode it dropped from 120 V to 77 V with reduction rates of 80% and 35%, respectively. The results showed that the charge dissipation rate of β-CD@PET was lower than that of blank PET under either low or high humidity. Notably, under low humidity, the charge dissipation rate of β-CD@PET was 10% lower than that of the blank PET film, which shows that the introduction of β-CD may increase the electrical storage of the PET film.

Fig. 6c and d show the charge decay of TENGs within 140 min. To measure the decay performance, we stopped the TENG operation process when it reached a stable and maximum value in the closed box with a controlled humidity of 15% or 95% RH. Then, the TENG was driven for one cycle to obtain the first I_{sc1} value and stopped again for 10 min for testing the next I_{sc2} value. During this process, no continuous friction of the triboelectrodes was applied to prevent obvious charge accumulation, and the whole process was carried out for 140 min to obtain a series of I_{sc} values. The results show that the I_{sc} of both blank PET- and β-CD@PET-based TENGs dropped to a stable value after 80 min at 15% RH, and the reduction rates were 27.3% and 21.6%. At 95% RH, the I_{sc} of the blank PET-based TENG decayed from 0.11 μA to 0.04 μA within 20 min with a reduction rate of 64%. However, the I_{sc} of the β-CD@PET-based TENG decayed to a stable value (16.0 μA) after 80 min

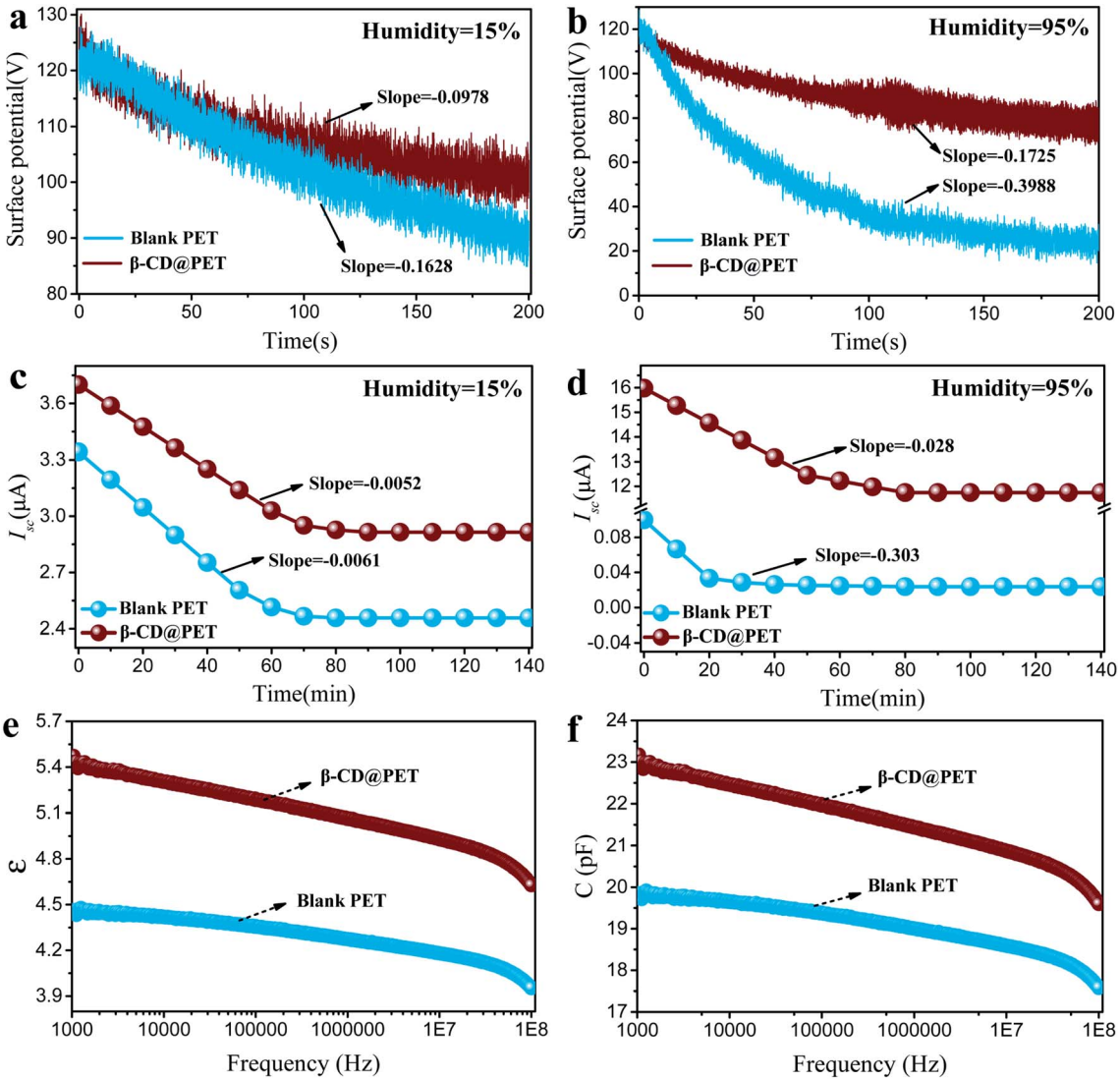

Fig. 6 Real-time surface potential of blank PET and β-CD@PET films at (a) 15% and (b) 95% RH. The charge decay test of (c) blank PET- and (d) β-CD@PET-based TENGs at 15% and 95% RH. A comparison of the (e) dielectric constant and (f) capacitance of blank PET and β-CD@PET films.

with a reduction rate of 27%. These results indicate that β-CD@PET has great charge retention ability, thus effectively slowing the decay of triboelectricity in a high-humidity environment.

In order to further explore the reasons for the increase in the charge storage capacity of the β-CD@PET film, the dielectric properties of the two PET films were tested, as shown in Fig. 6e and f. Compared with the blank PET film, the dielectric constant (ε) of the β-CD@PET film increased from 4.45 to 5.42 at 1000 Hz, indicating that the introduction of β-CD increases the triboelectric properties of the PET film itself. Moreover, the capacitance (C) of the PET film modified with β-CD increased from 19.8 pF to 22.9 pF at a frequency of 1000 Hz, which shows that the electricity storage performance of the β-CD@PET film has been improved.

Considering the excellent moisture resistance of the β-CD@PET film, it can be used as a friction layer of the TENG for energy harvesting under high humidity. As shown in Fig. 7a, several beakers filled with saturated KNO_3 solution were placed in a closed box to control the humidity at 95%. The motor was operated to make contact between the two electrodes of the β-CD@PET-PTFE-based TENG and then separate them to observe whether the LEDs connected to the TENG were lit up. The results show that the 248 LEDs connected to the β-CD@PET-based TENG were lit up at 95% RH, while the blank PET-based TENG can only light up 22 LEDs (Fig. 7b and c and Videos S1 and S2†). When LEDs were lit up at 95% RH, the I_{sc} of the blank PET-based TENG was 1.1 μA (Fig. 7f), while that of the β-CD@PET-based TENG was 15.3 μA, which is 14 times higher than that of the blank PET-based TENG. Then, the charging curves of the β-CD@PET-based TENG for different capacitors at 95% RH are shown in Fig. 7d. The results show that the β-CD@PET-based TENG can charge capacitors with capacitances of 2.2 μF, 4.7 μF and 10 μF at 95% RH, and within 62 s, the TENG can charge 10 V, 4.5 V and 1.2 V for 2.2 μF, 4.7 μF and 10 μF capacitors, respectively. Since the TENG outputs alternating

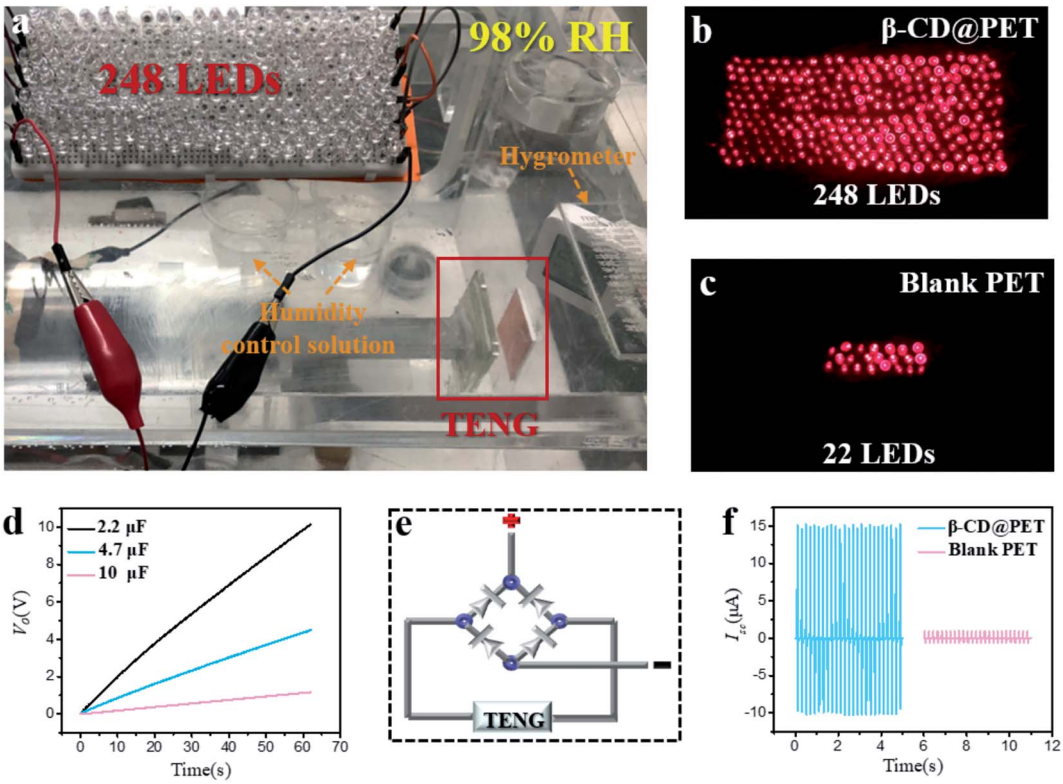

Fig. 7 (a) Schematic diagram of the lighting demonstration of β-CD@PET- and blank PET-based TENGs at 95% humidity, (b) β-CD@PET-based TENG lighting up 248 LEDs and (c) blank PET-based TENG lighting up 22 LEDs. (d) Charging curves for different capacitors, (e) diagram of the rectifier bridge and (f) I_{sc} of these two TENGs when lighting up LEDs at 95% RH.

current power, it needs to be integrated into direct current power to power the equipment, and the diagram of the rectifier bridge is shown in Fig. 7e.

In addition to being a power source for LEDs, the β-CD@PET-based TENG can also power small electronic devices, such as electronic watches, as shown in Fig. S8 and Video S3.† The environmental humidity in the closed box was controlled to 97% by using the saturated KNO_3 solution, and then the β-CD@PET electrode and PTFE electrode were placed in it for 24 h. When the motor drove the two electrodes of the TENG to make contact-separation movement, the electronic watch connected to the TENG worked normally, indicating that even at an extremely high humidity of 97%, the β-CD@PET-based TENG can still provide continuous high output.

Conclusion

In summary, we demonstrated a new type of β-CD@PET based TENG for mechanical energy collection with high output performance at high humidity, solving the output reduction of the solid–solid TENG with the increase of environmental humidity. The friction layer of this β-CD@PET based TENG is a PET film modified with β-CD whose surface is rich in hydroxyl groups that can form hydrogen bonds with water molecules in a high-humidity environment for fixing free water molecules on the surface of the film to form bound water and participate in the friction charging process. When the humidity increases from 15% to 95%, the output current of the TENG increases from 3.7 μA to 16 μA, showing an outstanding humidity resistance, and the higher the humidity, the greater the output. Moreover, the dielectric properties of the PET film increase due to the introduction of amino groups in β-cyclodextrin, which causes the I_{sc} of the TENG to increase by 3.7 times at 15% RH. This type of TENG has promising potential applications in energy harvesting, self-powered electronic devices, and early warning devices in fog, ocean, and other high humidity environments.

Author contributions

D. Wang and Z. Li conceived the project idea. N. Wang, Yizhe Liu and Y. Wu carried out the experiments. D. Wang organized and wrote the manuscript with input from all authors.

Conflicts of interest

There are no conflicts to declare.

Acknowledgements

The authors acknowledge the financial support from the Program for Taishan Scholars of Shandong Province (no. ts20190965), the National Key Research and Development Program of China (2020YFF0304600), the National Natural

Science Foundation of China (no. 51905518) and the Innovation Leading Talents Program of Qingdao (19-3-2-23-zhc) in China.

Notes and references

1 F. Fan, Z. Tian and Z. Wang, *Nano Energy*, 2012, **1**, 328–334.
2 C. Chen, H. Guo, L. Chen, Y. C. Wang, X. Pu, W. Yu, F. Wang, Z. Du and Z. L. Wang, *ACS Nano*, 2020, **14**, 4585–4594.
3 D. Tan, M. Willatzen and Z. L. Wang, *Nano Energy*, 2021, **79**, 105386.
4 W. Zhang, G. Gu, H. Qin, S. Li, W. Shang, T. Wang, B. Zhang, P. Cui, J. Guo, F. Yang, G. Cheng and Z. Du, *Nano Energy*, 2020, **77**, 105108.
5 X. Xia, H. Wang, H. Guo, C. Xu and Y. Zi, *Nano Energy*, 2020, **78**, 105343.
6 X. D. Yang, J. J. Han, G. Wang, L. P. Liao, C. Y. Xu, W. Hu, P. Li, B. Wu, A. M. Elseman, G. D. Zhou and Q. L. Song, *J. Mater. Sci.*, 2019, **54**, 9004–9016.
7 R. Lei, Y. Shi, Y. Ding, J. Nie, S. Li, F. Wang, H. Zhai, X. Chen and Z. L. Wang, *Energy Environ. Sci.*, 2020, **13**, 2178–2190.
8 Z. Li, J. Chen, J. Yang, Y. Su, X. Fan, Y. Wu, C. Yu and Z. L. Wang, *Energy Environ. Sci.*, 2015, **8**, 887–896.
9 K. i. Hiratsuka and Y. Meki, *Wear*, 2011, **270**, 446–454.
10 L. Li, X. Wang, P. Zhu, H. Li, F. Wang and J. Wu, *Nano Energy*, 2020, **70**, 104476.
11 V. Nguyen, R. Zhu and R. Yang, *Nano Energy*, 2015, **14**, 49–61.
12 X. Chen, L. Miao, H. Guo, H. Chen, Y. Song, Z. Su and H. Zhang, *Appl. Phys. Lett.*, 2018, **112**, 203902.
13 L. Gu, N. Cui, J. Liu, Y. Zheng, S. Bai and Y. Qin, *Nanoscale*, 2015, **7**, 18049–18053.
14 M. Zhang, Y. Jie, X. Cao, J. Bian, T. Li, N. Wang and Z. L. Wang, *Nano Energy*, 2016, **30**, 155–161.
15 S. Chen, C. Gao, W. Tang, H. Zhu, Y. Han, Q. Jiang, T. Li, X. Cao and Z. Wang, *Nano Energy*, 2015, **14**, 217–225.
16 Y. Feng, Y. Zheng, Z. U. Rahman, D. Wang, F. Zhou and W. Liu, *J. Mater. Chem. A*, 2016, **4**, 18022–18030.
17 Z. L. Wang, T. Jiang and L. Xu, *Nano Energy*, 2017, **39**, 9–23.
18 K. i. Hiratsuka and K. Hosotani, *Tribol. Int.*, 2012, **55**, 87–99.
19 H. Ryu, J.-H. Lee, T.-Y. Kim, U. Khan, J. H. Lee, S. S. Kwak, H.-J. Yoon and S.-W. Kim, *Adv. Energy Mater.*, 2017, **7**, 10700289.
20 X. Li, L. Zhang, Y. Feng, Y. Zheng, Z. Wu, X. Zhang, N. Wang, D. Wang and F. Zhou, *Adv. Funct. Mater.*, 2021, **31**, 2010220.
21 A. R. Mule, B. Dudem, S. A. Graham and J. S. Yu, *Adv. Funct. Mater.*, 2019, **29**, 1807779.
22 D. Li, C. Wu, L. Ruan, J. Wang, Z. Qiu, K. Wang, Y. Liu, Y. Zhang, T. Guo, J. Lin and T. W. Kim, *Nano Energy*, 2020, **75**, 104818.
23 M. Willatzen, L. C. Lew Yan Voon and Z. L. Wang, *Adv. Funct. Mater.*, 2020, **30**, 1910461.
24 Q. Zhou, K. Lee, K. N. Kim, J. G. Park, J. Pan, J. Bae, J. M. Baik and T. Kim, *Nano Energy*, 2019, **57**, 903–910.
25 R. Wen, J. Guo, A. Yu, J. Zhai and Z. l. Wang, *Adv. Funct. Mater.*, 2019, **29**, 1807655.
26 J. Shen, Z. Li, J. Yu and B. Ding, *Nano Energy*, 2017, **40**, 282–288.
27 C. Sun, Q. Shi, D. Hasan, M. S. Yazici, M. Zhu, Y. Ma, B. Dong, Y. Liu and C. Lee, *Nano Energy*, 2019, **58**, 612–623.
28 Z. Zhang, Z. Bai, Y. Chen and J. Guo, *Nano Energy*, 2019, **58**, 759–767.
29 W. J. Kim, V. Vivekananthan, G. Khandelwal, A. Chandrasekhar and S.-J. Kim, *ACS Appl. Electron. Mater.*, 2020, **2**, 3100–3108.
30 V. Vivekananthan, A. Chandrasekhar, N. R. Alluri, Y. Purusothaman and S.-J. Kim, *Nanoscale Adv.*, 2020, **2**, 746–754.
31 H. Yang, M. Wang, M. Deng, H. Guo, W. Zhang, H. Yang, Y. Xi, X. Li, C. Hu and Z. Wang, *Nano Energy*, 2019, **56**, 300–306.
32 G.-H. Lim, S. S. Kwak, N. Kwon, T. Kim, H. Kim, S. M. Kim, S.-W. Kim and B. Lim, *Nano Energy*, 2017, **42**, 300–306.
33 N. Wang, Y. Zheng, Y. Feng, F. Zhou and D. Wang, *Nano Energy*, 2020, **77**, 105088.
34 N. Wang, Y. Feng, Y. Zheng, L. Zhang, M. Feng, X. Li, F. Zhou and D. Wang, *Adv. Funct. Mater.*, 2021, **31**, 2009172.